Supporting Information

Highly Pure Silica Nanoparticles with High Adsorption Capacity obtained from Sugarcane Waste Ash

Suzimara Rovani,[†] Jonnatan J. Santos,[*,‡] Paola Corio[‡] and Denise A. Fungaro[†]

[†]Instituto de Pesquisas Energéticas e Nucleares (IPEN-CNEN/SP) - Av. Prof. Lineu Prestes, 2242, Cidade Universitária, 05508-000 São Paulo, SP, Brazil.

[‡]Instituto de Química, Universidade de São Paulo - Av. Prof. Lineu Prestes, 748, Cidade Universitária, P.O. Box 26077, 05508-000, São Paulo, SP, Brazil.

E-mail: jonnatan@iq.usp.br

Summary of Content

16 pages

5 equations: S1, S2, S3, S4, S5

7 tables: S1, S2, S3, S4, S5, S6, S7

11 figures: S1 (A) & (B) & (C) & (D), S2 (A) & (B) & (C), S3, S4, S5 (A) & (B) & (C), S6, S7 (A) & (B), S8, S9, S10 (insert in Fig. S10), S11

2 Schemes: Scheme S1, S2

Supplement: EDS and TEM of sugarcane waste ash and SiO_2NPs

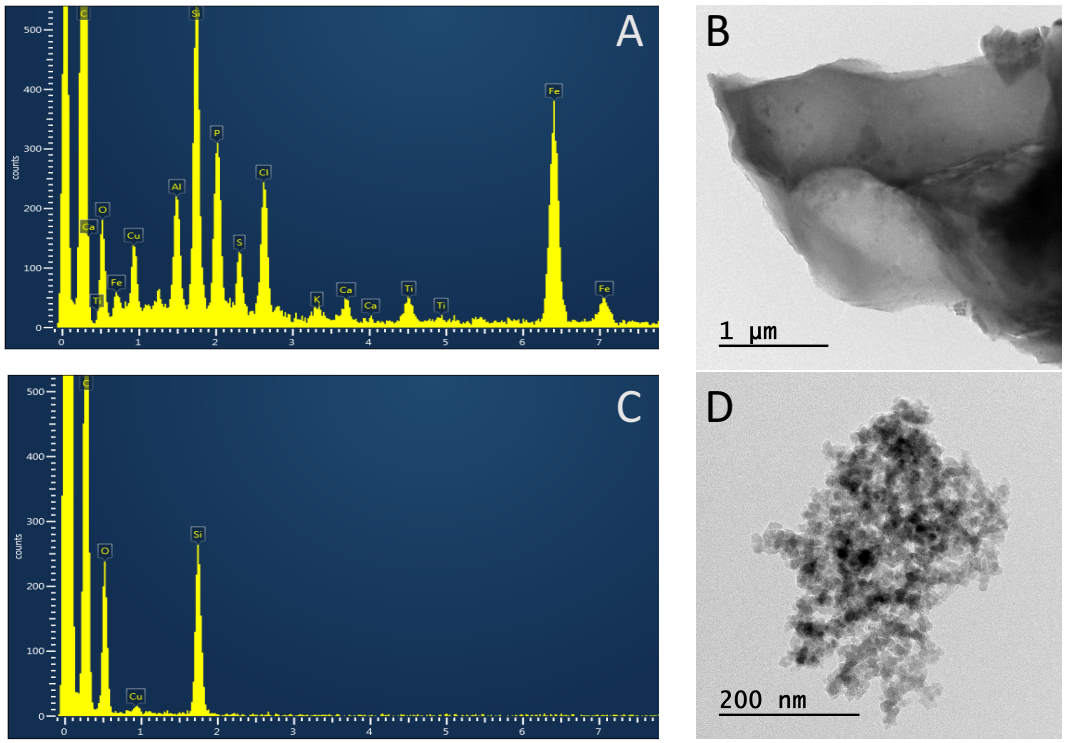

Figure S1. Sugarcane waste ash EDS (A) and TEM image (B) and silica nanoparticles EDS (C) and TEM image (D).

EDS of sugarcane waste ash shows the presence of several different elements (being Si, Fe, Al, P, Cl and S more abundant) and only Si and O were observed after silica nanoparticles synthesis procedure (Cu signal comes from TEM grid).

Supplement: Assignments of the IR vibrations

Table S1. Assignments of the IR vibrations of AO8 dye adsorption in the SiO_2NPs adsorbent.

Frequency (cm^{-1})	Assignment	References
2922	$\nu_{as}(CH_2)$ of CTAB	Zhang *et al.*[1]
2850	$\nu_{s}(CH_2)$ of CTAB	Zhang *et al.*[1]
1621	ν(-C=C-)	Ciric-Marjanovic *et al.*[2]
1554	ν_{as}(-COOH)	Konicki *et al.*[3]
1509	$\nu(CC)_{ar}$	Kowczyk-Sadowy *et al.*[4]
1490	$\nu(CC)_{ar}$	Kowczyk-Sadowy *et al.*[4]
1480	$\nu(CC)_{ar}$	Kowczyk-Sadowy *et al.*[4]
1468	$\nu(CC)_{ar}$	Kowczyk-Sadowy *et al.*[4]
1450	azo group (–N=N–)	Dent[5]
1199	phenolic -OH group δ(C-H) and δ(C-N)	Konicki *et al.*[6] Ciric-Marjanovic *et al.*[2]
1058	ν_{as}(Si–O–Si)	Boza *et al.*,[7] Hu and Hsieh[8]
1031	ν(O=S=O)	Dent[5] and Konicki *et al.*[6]
965	δ(OH) of silanol groups	Boza *et al.*,[7] Hu and Hsieh[8]
827	δ(C–H) of aromatic ring	Ciric-Marjanovic *et al.*[2]
799	ν_{s}(Si–O–Si)	Boza *et al.*,[7] Hu and Hsieh[8]
751	Out of plane deformation of ring	Kowczyk-Sadowy *et al.*[4]
722	δ(=C-H) of aromatic ring	Santos *et al.*[9]
689	Out of plane deformation of ring	Ciric-Marjanovic *et al.*[2]
641	In plane deformation of ring	Kowczyk-Sadowy *et al.*[4]
610	In plane deformation of ring	Kowczyk-Sadowy *et al.*[4]
603	In plane deformation of ring	Kowczyk-Sadowy *et al.*[4]
446	ν_{s}(Si–O–Si)	Boza *et al.*,[7] Hu and Hsieh[8]

*Symbols denotation: "ν" stretching; "δ" bending.

Supplement: TG analyses

The TG analyses were performed under oxygen atmosphere.

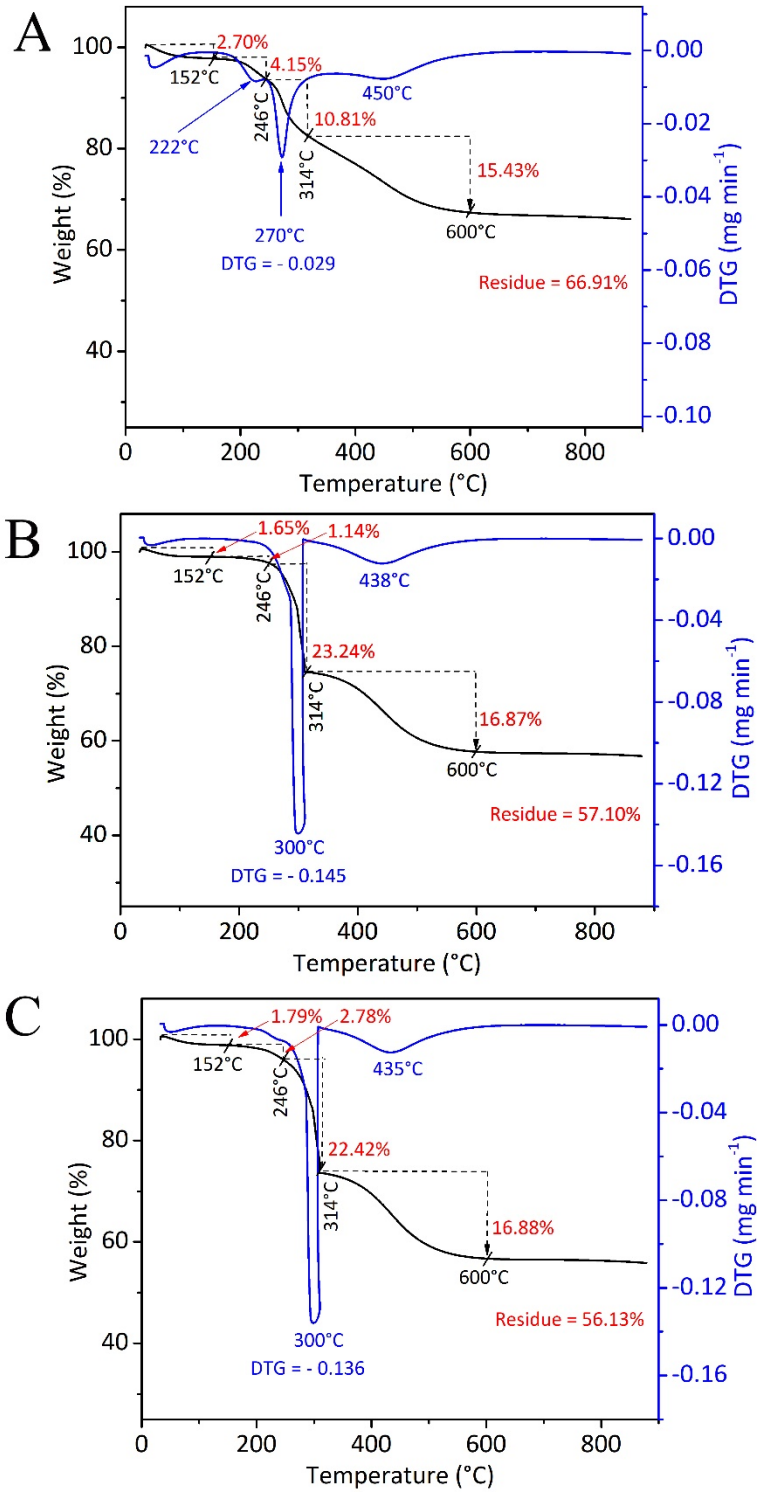

Figure S2. TG and DTG curves of (A) SiO_2NPs + AO8 (C_i = 75 mg L^{-1}), (B) SiO_2NPs + AO8 (C_i = 600 mg L^{-1}), and (C) SiO_2NPs + AO8 (C_i = 1000 mg L^{-1}).

Table S2. Thermogravimetric analyses of SiO_2NPs and SiO_2NPs after AO8 adsorption.

Samples	1ª wt. loss (%)	2ª wt. loss (%)	3ª wt. loss (%)	4ª wt. loss (%)	Residue (%)
	25-152°C	152-238°C	238-268°C	268-600°C	↑ 600°C
SiO_2NPs	3.08	6.55	14.82	10.81	64.74
	25-152°C	**152-246°C**	**246-314°C**	**314-600°C**	**↑ 600°C**
SiO_2NPs + dye (C_i 50 mg L^{-1})	3.85	4.19	9.63	12.38	69.95
SiO_2NPs + dye (C_i 75 mg L^{-1})	2.70	4.15	10.81	15.43	66.91
SiO_2NPs + dye (C_i 100 mg L^{-1})	2.28	3.83	11.70	18.22	63.97
SiO_2NPs + dye (C_i 150 mg L^{-1})	2.16	3.68	12.00	19.73	62.43
SiO_2NPs + dye (C_i 200 mg L^{-1})	1.99	2.70	17.63	16.13	61.55
SiO_2NPs + dye (C_i 400 mg L^{-1})	1.97	1.36	24.97	14.31	57.39
SiO_2NPs + dye (C_i 600 mg L^{-1})	1.65	1.14	23.24	16.87	57.10
SiO_2NPs + dye (C_i 1000 mg L^{-1})	1.79	2.78	22.42	16.88	56.13

Table S3. Thermogravimetric analyses of CTAB.

Sample	1ª wt. loss (%)	2ª wt. loss (%)	3ª wt. loss (%)	Residue (%)
	25-180°C	180-300°C	300-490°C	↑ 490°C
CTAB	0.00	86.55	12.41	1.04

Table S4. Thermogravimetric analyses of AO8 dye.

Sample	1ª wt. loss (%)	2ª wt. loss (%)	3ª wt. loss (%)	4ª wt. loss (%)	5ª wt. loss (%)	Residue (%)
	25-137°C	137-305°C	305-344°C	344-468°C	468-600°C	↑ 600°C
AO8	4.52	2.47	12.39	12.93	38.62	29.07

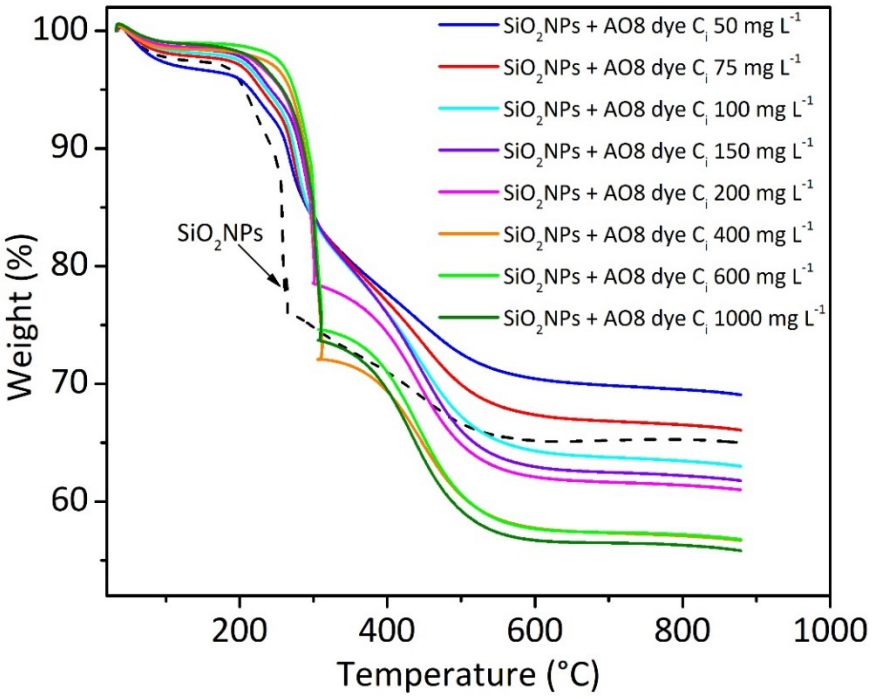

Figure S3. TG and DTG curves of SiO_2NPs, and SiO_2NPs + AO8 dye in different initial concentrations.

Supplement: FTIR analysis after TG analysis

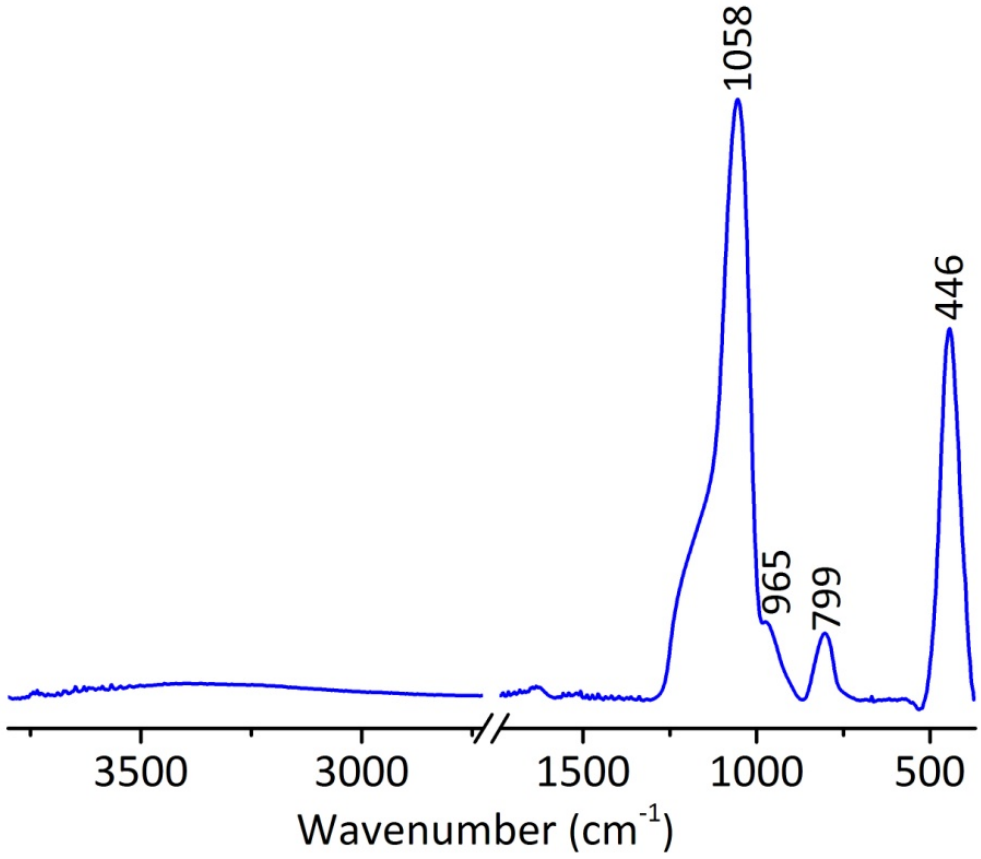

Figure S4. FTIR-ATR spectrum of the silica nanoparticles + AO8 dye (C_i = 200 mg L^{-1}) after TG analysis.

The residue of the sample (SiO_2NPs after AO8 adsorption) after TG analysis has only SiO_2NPs according to IR spectra Fig. S4.

Supplement: Kinetic AO8 adsorption for initial concentration 200 mg L^{-1}

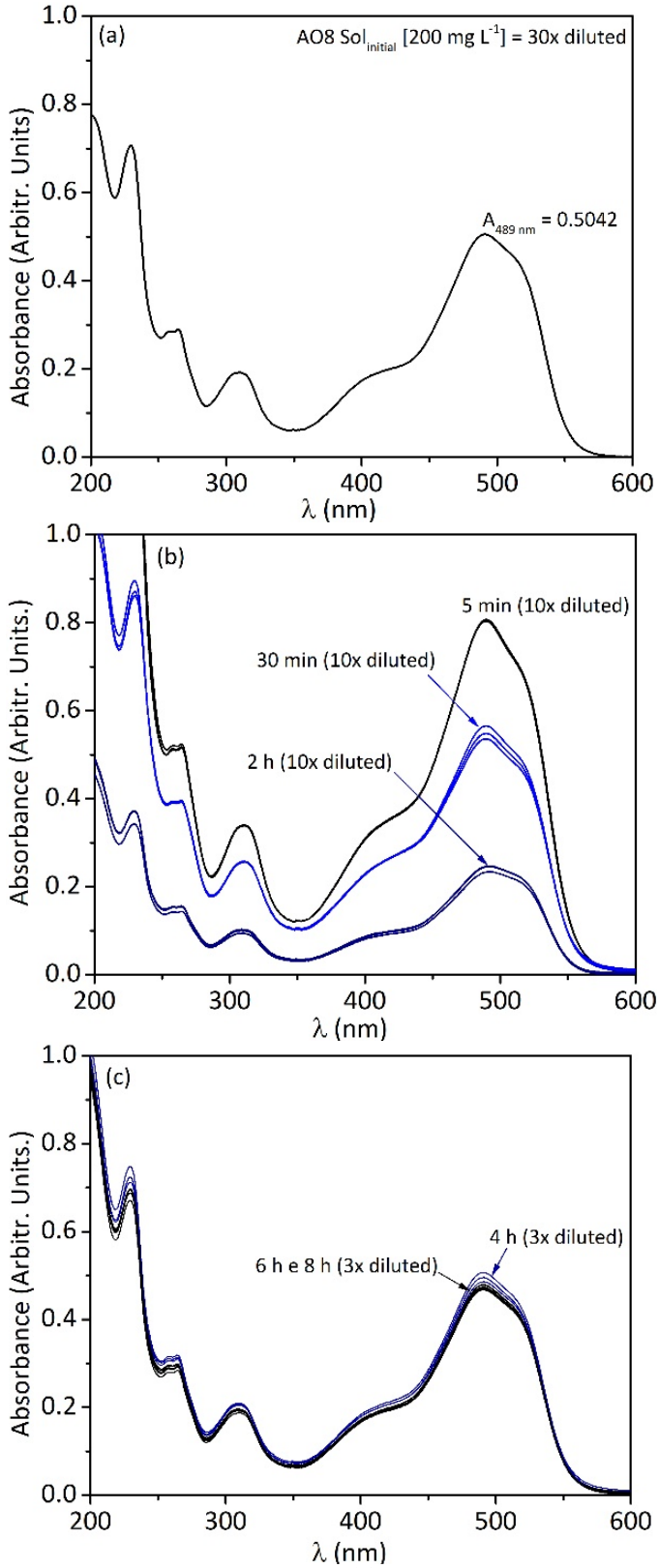

Figure S5. UV-Visible spectra before AO8 dye adsorption (a) initial solution 200 mg L^{-1}, after AO8 adsorption at 25 °C (b) 5-30 min and 2 h and (c) 4, 6 and 8 h. Samples in triplicate.

Supplement: Kinetic adsorption

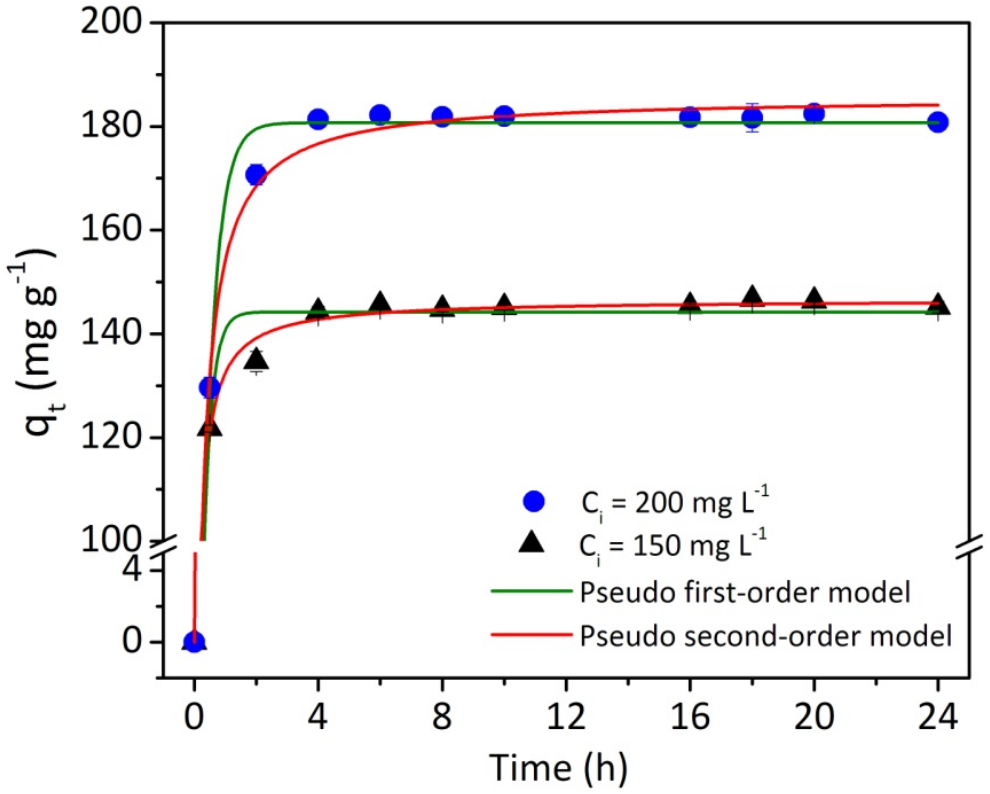

Figure S6. Pseudo first and pseudo second order model kinetics plot for the removal of AO8 by silica nanoparticles adsorbent. Conditions: 25°C, C_i = 150 and 200 mg L^{-1}, adsorbent mass 1.0 g L^{-1}.

Table S5. Kinetic parameters for the removal of AO8 by silica nanoparticles adsorbent.

Kinetic Parameters	C_i = 150 mg L^{-1}	C_i = 200 mg L^{-1}
Pseudo first-order		
k_1 (h^{-1})	3.70	2.49
q_e (mg g^{-1})	144	180
$R^2_{adj.}$	0.993	0.996
Pseudo second-order		
k_2 (g mg^{-1} h^{-1})	0.063	0.026
q_e (mg g^{-1})	146	185
$R^2_{adj.}$	0.998	0.997
Experimental Parameter		
q_e exp. (mg g^{-1})	145	182

Supplement: Equilibrium adsorption

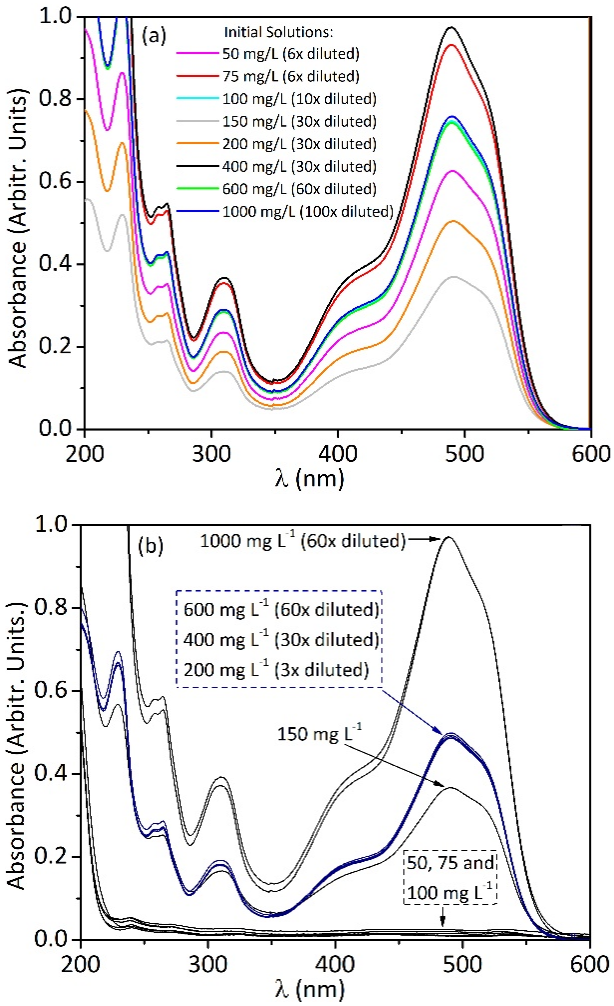

Figure S7. UV-Visible spectra before AO8 dye adsorption (a) initial solutions at concentrations from 50 to 1000 mg L^{-1}, after AO8 adsorption at equilibrium time 4 h (b) 25°C isotherm. Samples in triplicate.

Table S6. Equilibrium parameters for the removal of AO8 by silica nanoparticles adsorbent.

Equilibrium Parameters	25°C	35°C	45°C
Langmuir			
Q_{max} (mg g^{-1})	187	-	-
K_L (L mg^{-1})	5.79	-	-
$R^2_{adj.}$	0.889	-	-
Freundlich			
K_F (mg g^{-1} (mg L^{-1})$^{-1/nF}$)	109	-	-
n_F	9.25	-	-
$R^2_{adj.}$	0.952	-	-
Liu			
Q_{max} (mg g^{-1})	230	228	233
K_g (L mg^{-1})	1.19	1.29	0.893
n_L	0.346	0.381	0.378
$R^2_{adj.}$	0.991	0.978	0.979

Supplement: AO8 adsorption time for initial concentration 20 mg L^{-1}

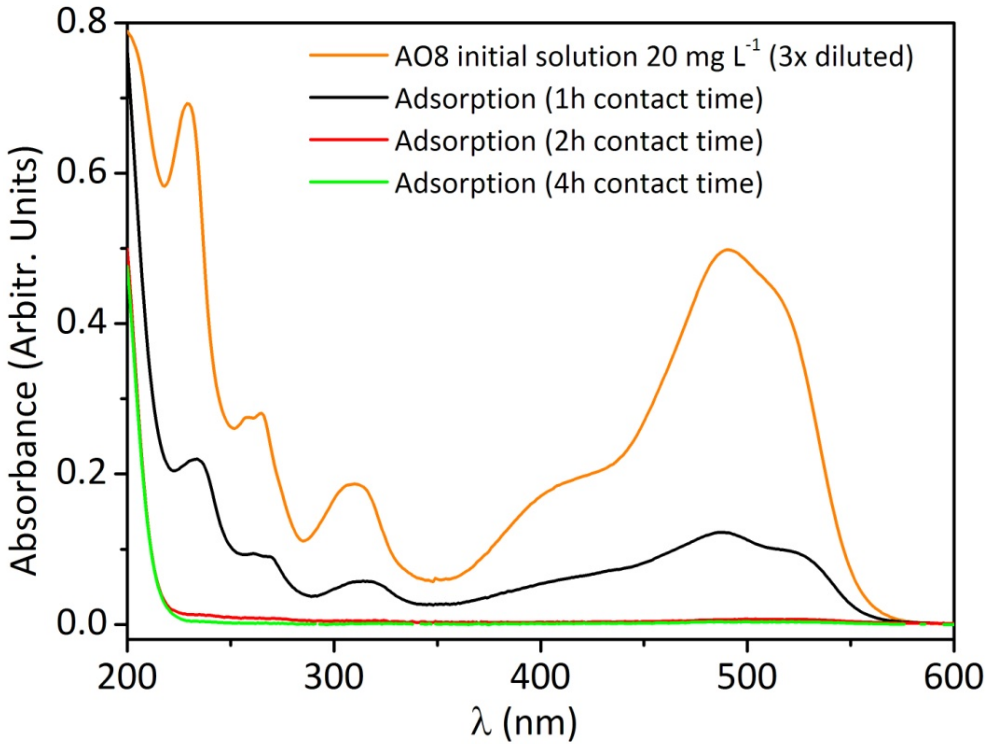

Figure S8. UV-Visible spectra before AO8 dye adsorption (orange line) initial solution 20 mg L^{-1} and after AO8 adsorption at 25°C (black line) 1 h contact time; (red line) 2h contact time; and (green line) 4h contact time.

For low concentrations of AO8 dye a shorter contact time (2 h) between adsorbate-adsorbent is sufficient to adsorb all dye.

Supplement: SiO_2NPs reuse cycles

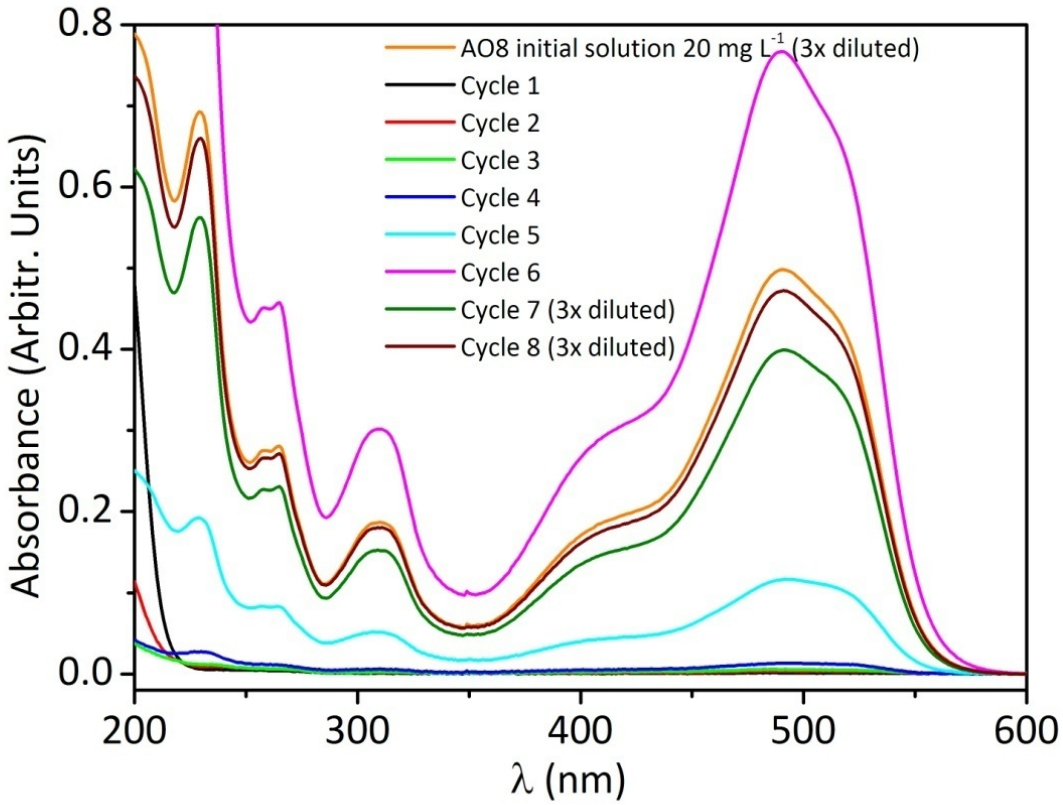

Figure S9. UV-Visible spectra before AO8 dye adsorption (orange line) initial solutions 20 mg L^{-1}, and reuse cycles of SiO_2NPs after AO8 adsorption, C_i = 20 mg·L^{-1} at 25°C for 2h, adsorbent mass 1.0 g L^{-1}.

Supplement: Analytical curve

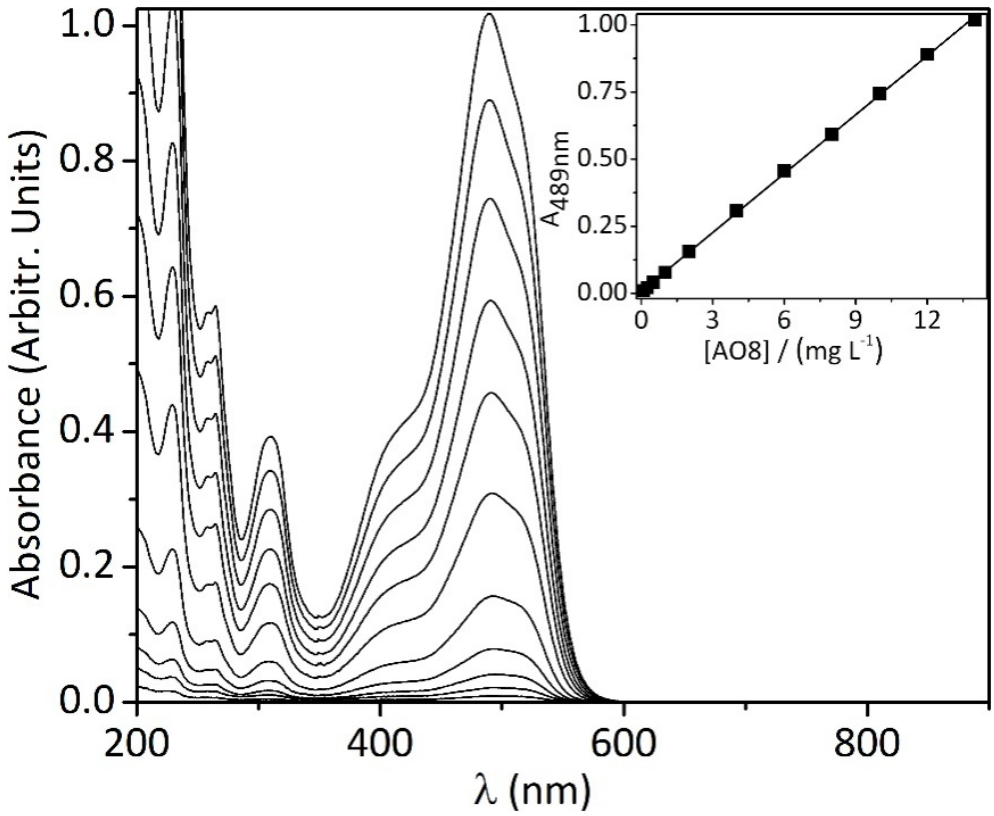

Figure S10. UV-Visible spectra of solution containing AO8 dye at concentrations from 0.10 to 14.00 mg L^{-1}. Insert: analytical curve of AO8 dye.

The equation of the analytical curve (insert in Fig. S10) was A = 0.00732 + 0.07315. [AO8] (mg L^{-1}), and the value of the coefficient of determination adjusted ($R^2_{adj.}$) was 0.99963.

Supplement: Physical and chemical properties of Acid Orange 8

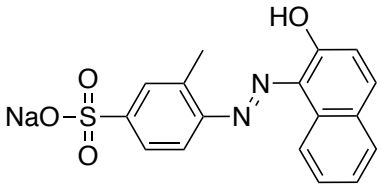

Figure S11. Chemical structure of Acid Orange 8.

Table S7. Physical and chemical properties of Acid Orange 8.

Physico-Chemical Properties	
Chemical formula	$C_{17}H_{13}N_2NaO_4S$
Molecular weight	364.35 g mol^{-1}
Structure	Azo
CAS number	5850-86-2
Color index number	15575
Dye content	65 %
λ_{max} (nm)	490 nm

Supplement: Kinetic and equilibrium adsorption models

Kinetic adsorption

Kinetic adsorption models used in this publication were pseudo-first order (Eq. S1) and pseudo-second order (Eq. S2).

$$q_t = q_e.\left(1 - e^{(-k_1 t)}\right) \quad \text{(Eq. S1)}$$

$$q_t = \frac{k_2 . q_e^2 \ t}{1 + \ k_2 . q_e . t} \quad \text{(Eq. S2)}$$

Where in the Eq. S1, q_t is the amount of adsorbate adsorbed at time t (mg g^{-1}), q_e is the equilibrium adsorption capacity (mg g^{-1}), k_1 is the pseudo-first-order rate constant (h^{-1}), and t is the contact time (h). Eq. S2, k_2 is the pseudo-second-order rate constant (g mg^{-1} h^{-1}).[10-13]

Equilibrium adsorption

Equilibrium adsorption models utilized were Langmuir[14] (Eq. S3); Freundlich[15] (Eq. S4) and Liu[11] (Eq. S5).

$$q_e = \frac{Q_{max} . K_L . C_e}{1 + \ K_L . C_e} \quad \text{(Eq. S3)}$$

$$q_e = K_F . C_e^{\frac{1}{n_F}} \quad \text{(Eq. S4)}$$

$$q_e = \frac{Q_{max} . (K_g . C_e)^{n_L}}{1 + \ (K_g . C_e)^{n_L}} \quad \text{(Eq. S5)}$$

Where for Eq. S3, q_e is the amount of adsorbate adsorbed at the equilibrium (mg g^{-1}), C_e is the adsorbate concentration at the equilibrium, i.e., C_e is the adsorbate concentration residual on solution (mg L^{-1}), K_L is the Langmuir equilibrium constant (L mg^{-1}), and Q_{max} is the maximum adsorption capacity of the adsorbent (mg g^{-1}) assuming the formation of a monolayer of adsorbate over adsorbent.[10]

For Eq. S4, K_F is the Freundlich equilibrium constant (mg g^{-1}(mg L^{-1})$^{-1/nF}$), n_F is the Freundlich exponent (dimensionless) and C_e is the adsorbate concentration residual on solution (mg L^{-1}). [10]

For Eq. S5, K_g is the Liu equilibrium constant (L mg^{-1}); n_L is dimensionless exponent of the Liu equation; Q_{max} is the maximum adsorption capacity of the adsorbent (mg g^{-1}), C_e is the adsorbate concentration residual on solution (mg L^{-1}) and n_L could assume any positive value. Liu model predicts that the active sites of the adsorbent cannot assume the same energy.[10-11]

Scheme 1. Preparation of Sodium Silicate Solution from SWA.

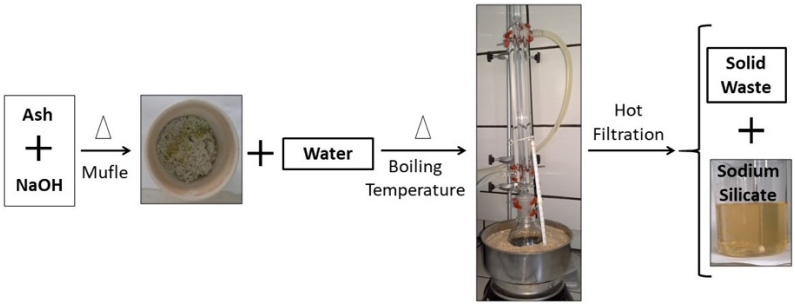

Scheme 2. Surfactant mediated synthesis of silica nanoparticles (SiO_2NPs) from the obtained sodium silicate.

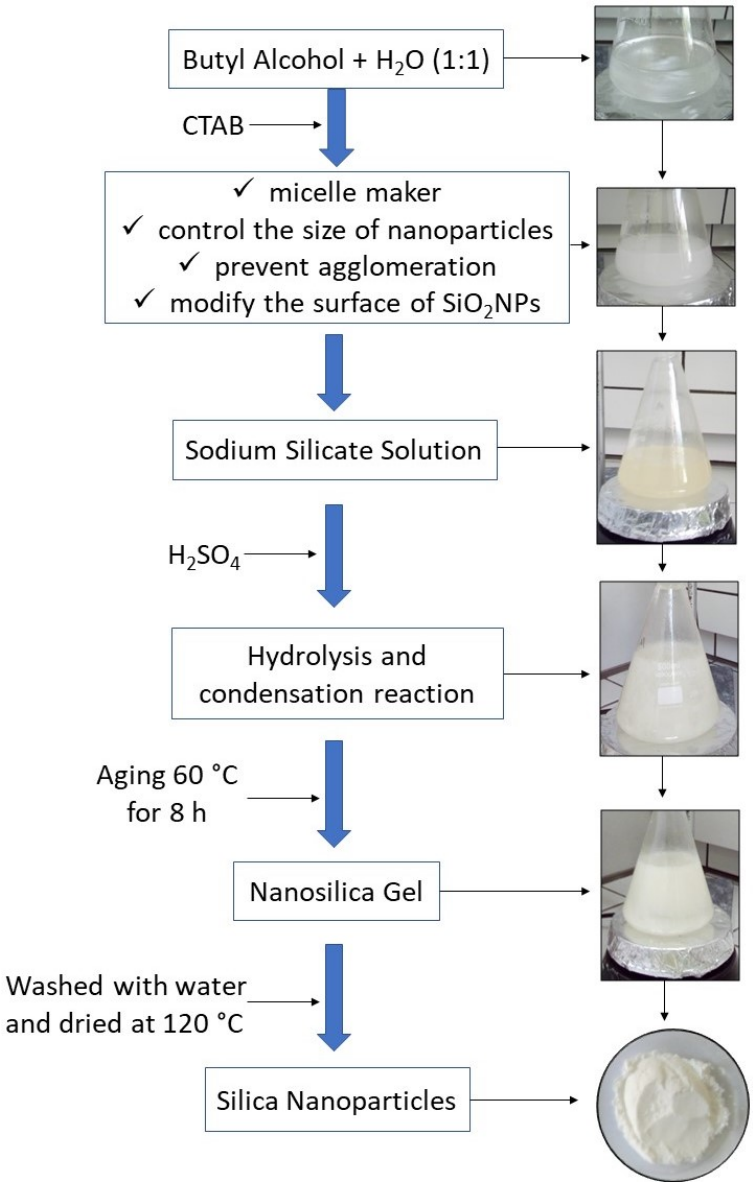

Supplementary References

(1) Zhang, T.; Xu, G.; Puckette, J.; Blum, F. D., Effect of Silica on the Structure of Cetyltrimethylammonium Bromide. *J. Phys. Chem. C* **2012,** *116* (21), 11626-11634.

(2) Ćirić-Marjanović, G.; Mentus, S.; Pašti, I.; Gavrilov, N.; Krstić, J.; Travas-Sejdic, J.; Strover, L. T.; Kopecká, J.; Moravková, Z.; Trchová, M.; Stejskal, J., Synthesis, Characterization, and Electrochemistry of Nanotubular Polypyrrole and Polypyrrole-Derived Carbon Nanotubes. *J. Phys. Chem.: C* **2014,** *118* (27), 14770-14784.

(3) Konicki, W.; Aleksandrzak, M.; Moszynski, D.; Mijowska, E., Adsorption of anionic azo-dyes from aqueous solutions onto graphene oxide: Equilibrium, kinetic and thermodynamic studies. *J. Colloid Interface Sci.* **2017,** *496*, 188-200.

(4) Kowczyk-Sadowy, M.; Świsłocka, R.; Lewandowska, H.; Piekut, J.; Lewandowski, W., Spectroscopic (FT-IR, FT-Raman, 1H- and 13C-NMR), Theoretical and Microbiological Study of trans o-Coumaric Acid and Alkali Metal o-Coumarates. *Molecules* **2015,** *20* (2), 3146-3169.

(5) Dent, G., Vibrational Spectroscopy of Colors, Dyes and Pigments. In *Handbook of Vibrational Spectroscopy*, John Wiley & Sons, Ltd: 2006.

(6) Konicki, W.; Cendrowski, K.; Chen, X.; Mijowska, E., Application of hollow mesoporous carbon nanospheres as an high effective adsorbent for the fast removal of acid dyes from aqueous solutions. *Chem. Eng. J.* **2013,** *228* (Supplement C), 824-833.

(7) Boza, A. F.; Kupfer, V. L.; Oliveira, A. R.; Radovanovic, E.; Rinaldi, A. W.; Meneguin, J. G.; Domingues, N. L. C.; Moisés, M. P.; Favaro, S. L., Synthesis of α-aminophosphonates using a mesoporous silica catalyst produced from sugarcane bagasse ash. *RSC Adv.* **2016,** *6* (29), 23981-23986.

(8) Hu, S. X.; Hsieh, Y. L., Preparation of Activated Carbon and Silica Particles from Rice Straw. *ACS Sustain. Chem. Eng.* **2014,** *2* (4), 726-734.

(9) Santos, R. M. M. d.; Gonçalves, R. G. L.; Constantino, V. R. L.; Santilli, C. V.; Borges, P. D.; Tronto, J.; Pinto, F. G., Adsorption of Acid Yellow 42 dye on calcined layered double hydroxide: Effect of time, concentration, pH and temperature. *Appl. Clay Sci.* **2017,** *140*, 132-139.

(10) Lima, É. C.; Adebayo, M. A.; Machado, F. M., Kinetic and Equilibrium Models of Adsorption. In *Carbon Nanomaterials as Adsorbents for Environmental and Biological Applications*, Bergmann, C. P.; Machado, F. M., Eds. Springer International Publishing: Cham, 2015; pp 33-69.

(11) Liu, Y.; Liu, Y.-J., Biosorption isotherms, kinetics and thermodynamics. *Sep. Purif. Technol.* **2008,** *61* (3), 229-242.

(12) Ho, Y.-S., Review of second-order models for adsorption systems. *J. Hazard. Mater.* **2006,** *136* (3), 681-689.

(13) Ho, Y.-S., Using of "pseudo-second-order model" in adsorption. *Environ. Sci. Pollut. Res.* **2014,** *21* (11), 7234-7235.

(14) Langmuir, I., THE ADSORPTION OF GASES ON PLANE SURFACES OF GLASS, MICA AND PLATINUM. *J. Am. Chem. Soc.* **1918,** *40* (9), 1361-1403.

(15) Freundlich, H. M. F., Over the Adsorption in Solution. *J. Phys. Chem.* **1906,** *57*, 385-471.